

Novel biotinylated bile acid amphiphiles: Micellar aggregates formation and interaction with hepatocytes†

Luca Rizzi,^a Marta Braschi,^a Miriam Colombo,^{b,c} Nadia Vaiana,^a Gianpaolo Tibolla,^d Giuseppe Danilo Norata,^d Alberico Luigi Catapano,^d Sergio Romeo^{*a} and Davide Proserpi^{*b,c}

Received 13th October 2010, Accepted 4th February 2011

DOI: 10.1039/c0ob00878h

Amphiphilic bile acids linked through an oligoethylene glycol to a biotin moiety were synthesized and shown to create micellar structures in aqueous environment, interact with avidin and be efficiently incorporated into hepatocyte cells, suggesting their potential as a drug delivery system against liver diseases.

Introduction

The success of a drug therapy derives from the achievement of effective drug concentrations at the target site. However, this goal is often complicated by several factors, including those related to physical properties of the active ingredient, such as water solubility, membrane permeability and metabolic stability. Because of the difficulties associated with drug therapy, the design of new delivery systems remains a great challenge in medicinal chemistry. Vehicles include nanoparticles,¹ microcapsules,² liposomes,³ and micelles.⁴ The decoration of nanoparticle surfaces with molecules capable of targeting a specific cell type or tissue (e.g. antibodies, saccharides or peptides), is essential to develop an efficient delivery system.^{5,6} In addition, such nanosystems should be non-toxic, biocompatible, possibly easy to synthesize, stable and possessing long half-life in biological fluids.

Among the human organs, the liver plays a primary role in the protection of organisms by assault of xenobiotics and in the synthesis of blood plasma components. For these reasons hepatic diseases, such as hepatitis, cirrhosis and liver cancers, represent a serious problem for human health.^{7–9} A crucial step for a successful treatment of hepatic diseases is the need to reduce side effects, which might be achieved by using nanostructures containing molecules able to selectively interact with specific hepatocyte membrane receptors.

Within this effort, we describe here the synthesis and the structural characterization of biotinylated bile acid amphiphiles (BBAA, **1–4**, Fig. 1) containing, in the lipophilic region, different bile acids, namely cholic acid **1** (CA), deoxycholic acid **2** (DCA), ursodeoxycholic acid **3** (UDCA) and lithocholic acid **4** (LA). Bile acids are recognized by specific transport systems on hepatocyte membranes^{10,11} and this property has made them excellent molecules to be included in liver drug targeting systems.^{12,13} Moreover, the presence of bile acids, such as UDCA, may itself be valuable, because UDCA is an hepatoprotector that stabilizes the liver membrane in cholestatic injury.¹⁴ Biotinylated lithocholic acids have been demonstrated to inhibit mammalian DNA polymerases.¹⁵ In this work, biotin and bile acids were linked by an oligoethyleneglycol (OEG-8) chain selected for its biocompatibility and because OEG-8 was demonstrated to

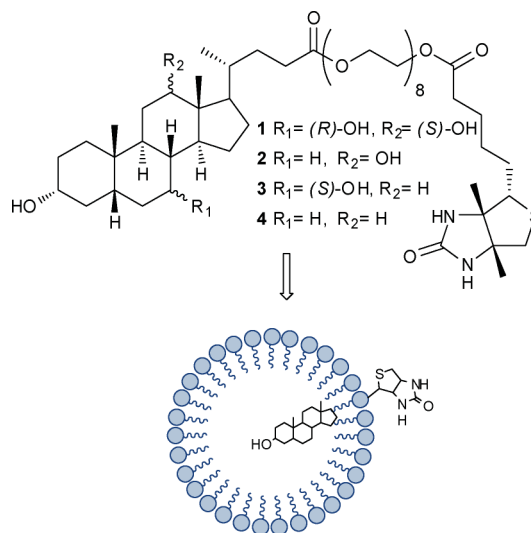


Fig. 1 Synthesized BBAA and a schematic representation of the orientation of bile acid and biotin in micelles.

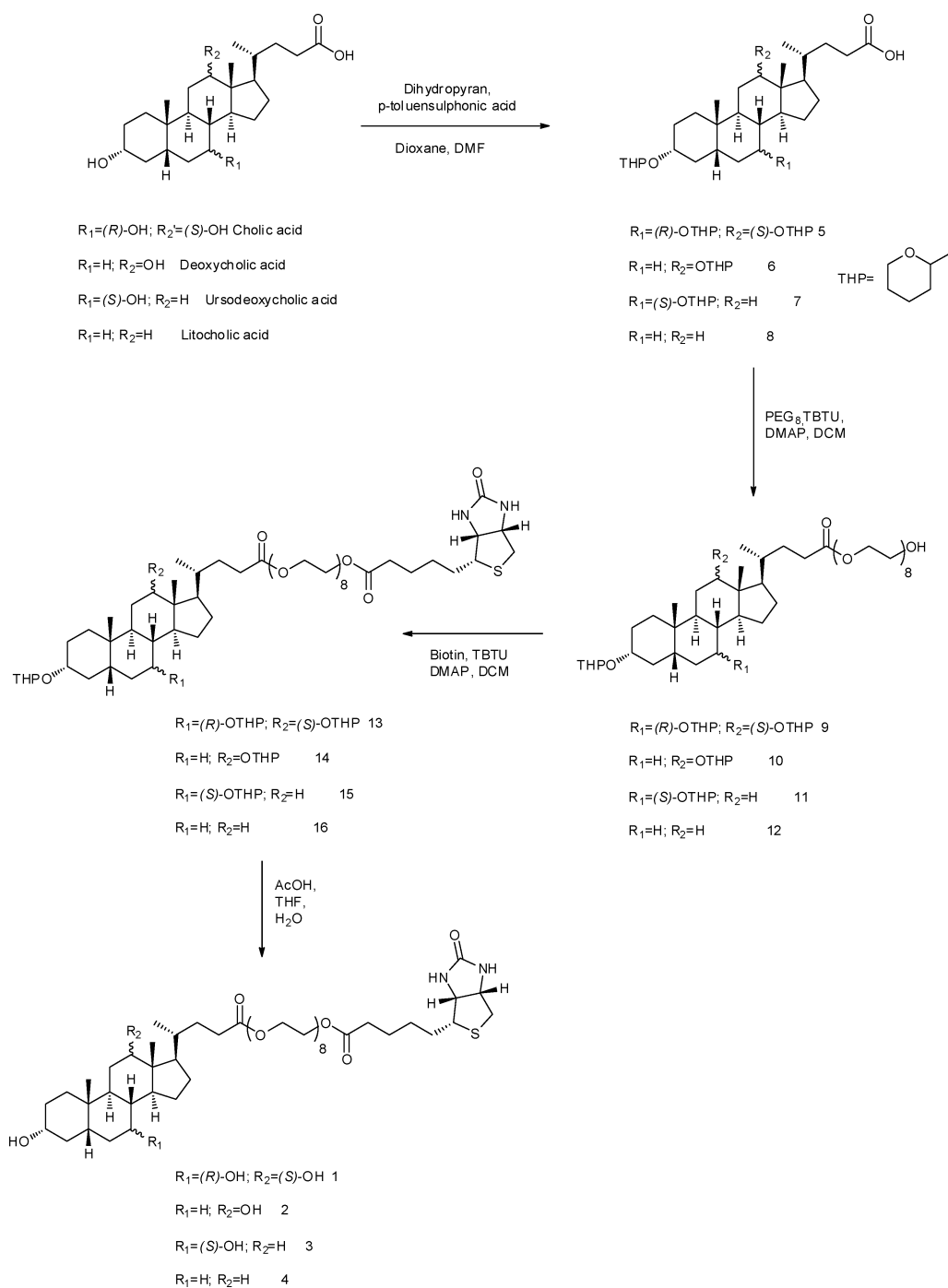
^aDipartimento di Scienze Farmaceutiche "Pietro Pratesi", Università degli Studi di Milano, 20133, Milano, Italy. E-mail: sergio.romeo@unimi.it; Fax: (+39)02503 19359; Tel: (+39)02503 19363

^bDipartimento di Biotecnologie e Bioscienze, Università di Milano-Bicocca, P.zza della Scienza 2, 20126, Milano, Italy. E-mail: davide.proserpi@unimib.it; Fax: (+39)026448 3565; Tel: (+39)02644 83302

^cCentro di Microscopia Elettronica per le nanotecnologie applicate alla medicina (CMENA), Università di Milano, Via G.B. Grassi 74, 20157, Milano, Italy

^dDipartimento di Scienze Farmacologiche, Università degli Studi di Milano, 20133, Milano, Italy

† Electronic supplementary information (ESI) available: Supplementary spectra, figures and tables. See DOI: 10.1039/c0ob00878h



Scheme 1 Synthesis of biotinylated bile acid amphiphiles.

positively affect cell permeability and to increase the nanoparticle concentration in target tissues.^{16–18}

Results and discussion

BBAA 1–4 were synthesized by two sequential esterification couplings with OEG-8 and biotin, respectively (Scheme 1). Because of the reactivity of the hydroxyl groups of bile acids, a preliminary OH-protection with dihydropyran was needed (compounds 5–8, Scheme 1).¹⁹

These molecules were assessed in water as to their tendency to form micellar aggregates spontaneously. Table 1 summarizes the fundamental micelle properties for 1–4. The order in water solubility was $1 > 2 \geq 3 > 4$, which inversely reflects the ability of forming aggregates as determined by the respective CMC values.

The ability of BBAA 1–4 to self-associate forming micellar aggregates in aqueous phase was determined by fluorescence analysis using pyrene as a probe.^{12,20–24} In Fig. S1 (ESI[†]), the pyrene excitation spectra at various concentrations of 1–4 are shown.

Table 1 Micelles characterization

	1	2	3	4
Water solubility (mg mL ⁻¹)	2.0	1.0	1.0	0.5
CMC (mol L ⁻¹) ^a	n.m.f. ^c	1.2 × 10 ⁻³	7.5 × 10 ⁻⁵	1.2 × 10 ⁻⁵
Average <i>d</i> (nm) ^b	n.m.f. ^c	122 ± 7	140 ± 11	82 ± 5

^a Calculated by pyrene excitation spectra. ^b Diameter determined by dynamic light scattering. ^c No micelle formation.

In the pyrene excitation spectra of **1**, no shift of pyrene spectra was observed, suggesting that the CA-(OEG-8)-biotin conjugate is not able to create micelles in water. In contrast, the spectra of **2–4** show a gradual shift of pyrene from 333.5 to 337.5 nm for **2**, from 334.0 to 337.0 nm for **3**, and from 334.0 to 338.0 nm for **4**, typical of the formation of micelles in water. The shift of pyrene spectra was recorded in solutions at concentrations higher than 10⁻² g L⁻¹. By plotting the values of $I_{337.5}/I_{333.5}$ for **2**, I_{337}/I_{334} for **3** and I_{338}/I_{334} for **4** vs. the logarithm of concentration, it was possible to obtain a distribution curve of the respective micelle formation (Fig. 2), which was used to determine the CMC values of **2–4** (Table 1). Dynamic light scattering (DLS) was used to confirm the presence of micelles or larger aggregates and to determine the relevant hydrodynamic sizes (Fig. S2, ESI[†]),

which were in the same order of other recent observations.²⁵ In particular, previous evidence supports the idea that bile acids derivatives tend to form multimicellar aggregates in concentrated solutions.²⁶ Micelles from BBAA showed long-term stability in water. The DLS distributions of **2–4** dispersions after 1 month are reported in the ESI[†] (Fig. S3). A size increment within 20% and the maintenance of a narrow size distribution provided evidence on the BBAA aggregate stability.

An insight into the molecular features of **1–4** evidenced that aggregate formation could be associated with the number of hydroxyl functionalities. In fact, while compound **1** containing 3 OH groups was unable to create assemblies, compound **4**, which contains only one free hydroxyl, exhibited a strong propensity to form micelles in aqueous media, as confirmed by the low experimental CMC. BBAA **2** and **3** were also able to self-assemble into organized structures, but these structures were remarkably larger than those formed from **4**, as these compounds hold 2 hydroxyl groups, giving an intermediate hydrophilic character between **1** and **4**. Comparing CMC values of **2** and **3** suggested that the aggregate formation should be more favored by the presence of hydroxyl group at 7 rather than at 12 position in the cyclopentane perhydrophenantrenic ring.

Since biotin (bt) was present in all BBAA, we have tested the ability of these molecules to bind avidin (Av). Av–bt interaction, indeed, could be very useful in pretargeting approaches to cancer

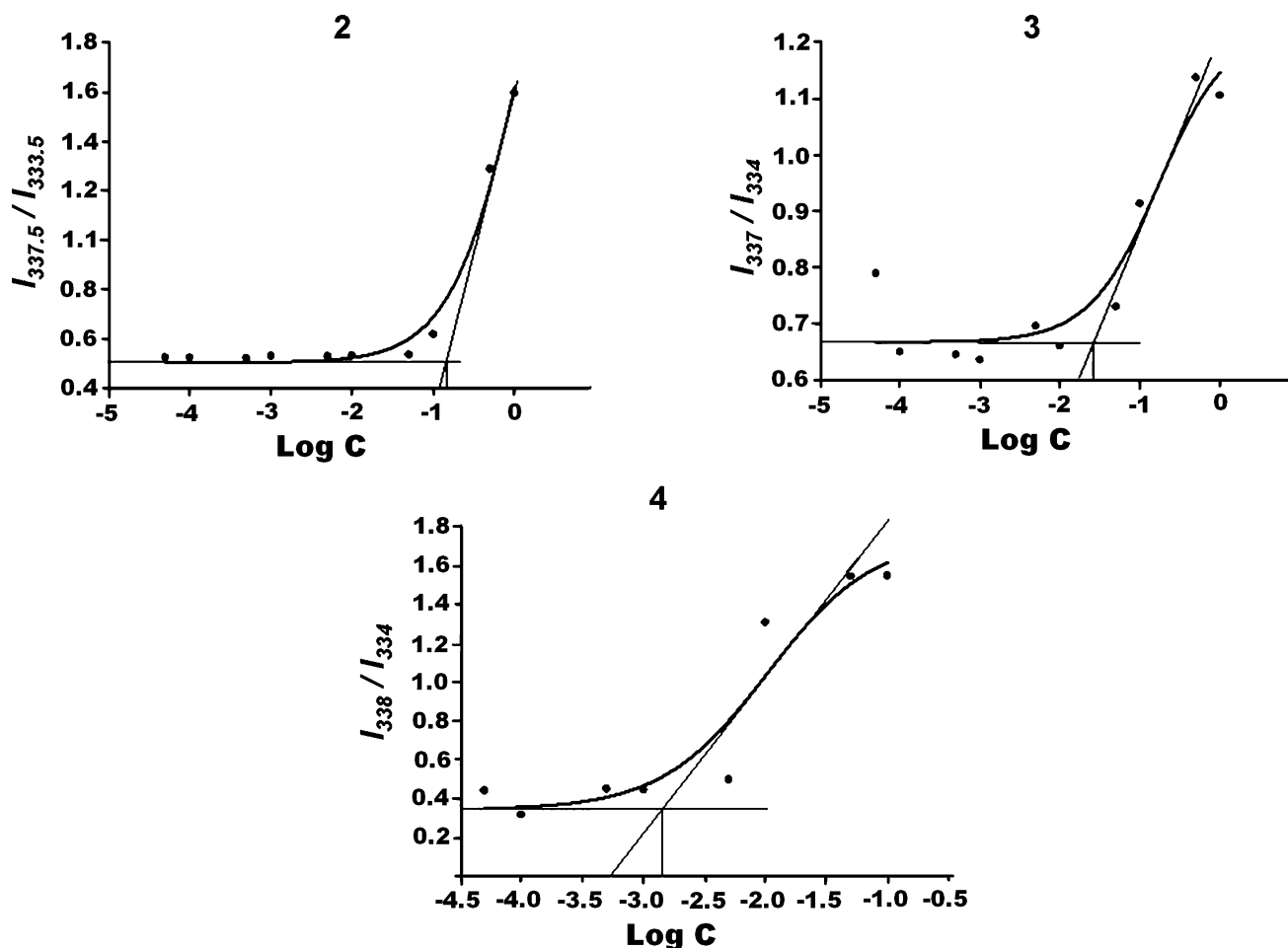


Fig. 2 Plot of $I_{337.5}/I_{333.5}$ (**2**), I_{337}/I_{334} (**3**) and I_{338}/I_{334} (**4**) vs. log *C* for **2**, **3** and **4** at 25 °C.

and inflammatory diseases.²⁷ The affinity of **1–4** towards Av was assessed using a spectrophotometric assay.²⁸ The Green method is based on monitoring 4-hydroxyazobenzene-2-carboxylic acid (HABA), which binds to Av and can be used as an indicator of binding sites occupied by bt.²⁹ Fig. 3a shows the concentration and the percentage of saturated Av binding sites.

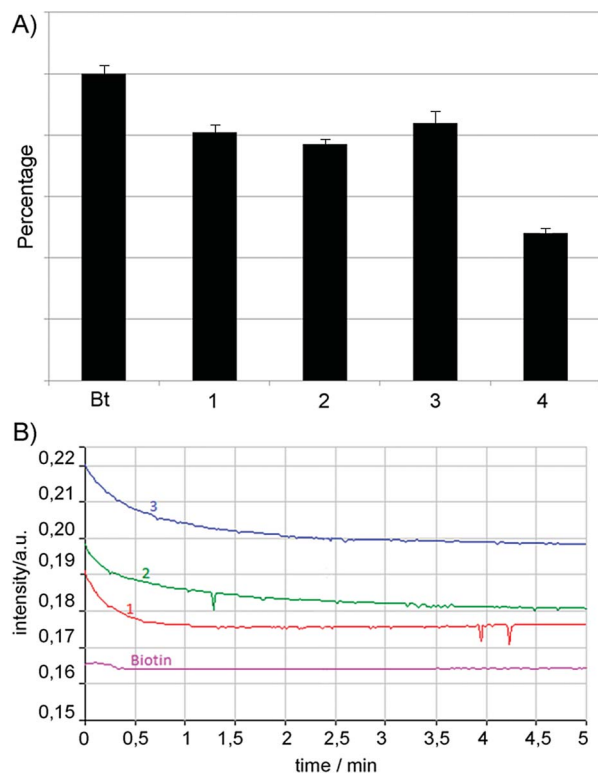


Fig. 3 A) Percentage of Av binding sites occupied by bt and BBAA **1–4**. B) Progress of binding between Av-bt and Av-BBAA **1–3** vs. time.

BBAA **1–3** exhibited an affinity for Av comparable to that of free bt used as control. BBAA **4**, however, provided an apparent lower affinity because it was not possible to prepare the optimal solution (2 mM) necessary for the assay, as the concentration required was higher than the maximal solubility of this compound (1 mM). Hence, although the quantitative data for **4** were considered unreliable, we could conclude that, because of the similarity with the other molecules, **4** was also able to bind Av. Fig. 3b shows the time dependence of formation of the Av-bt complex for **1–3**. Compound **1** could saturate Av within 1 min, similar to free

bt (0.5 min), while **2** and **3** were 5 times slower. The remarkable difference in the rate of formation of a stable complex with Av might be explained in terms of the different molecular state in solution, which would result in lower rates when amphiphiles are assembled into micelles. We can assume that the bt of amphiphilic compounds which form micelles at first should be not able to interact with Av because they are engaged directly in micelle formation. Only after the micelles have been completely formed and bt is in contact with water, does it become able to bind Av. This assumption was confirmed by the behaviour of compound **1**, which, being unable to form micelles, was found to bind Av in a time on the same order of free bt. In order to evaluate whether the complex formation would occur involving entire micelles or whether the binding with Av would induce the aggregate disruption, a spectrofluorimetric assay was undertaken. A solution of pyrene was added in parallel to two samples, each with a concentration of 1.0 mg mL⁻¹ for compounds **2** and **3** and of 0.5 mg mL⁻¹ for **4**, higher than CMC.²¹ To the first sample was added a solution of Av (0.1 mg mL⁻¹) in order to reach a 1 : 20 Av/bt ratio whereas to the second was added Av to reach a 1 : 100 Av/bt ratio.

In Fig. 4, the band of pyrene resulted in different peaks depending on Av concentration. In particular, 1) the first sample (band 3, red, 1 : 20 Av/bt ratio) was detected as a peak at 333.5 nm for **2**, 333.8 nm for **3** and 334.7 nm for **4**, typical of free pyrene in solution (band 1, black), suggesting that high concentrations of Av may lead to micelle disruption; 2) the second sample (band 4, green, 1 : 100 Av/bt ratio) displays a peak at 336.6 nm for **2**, 336.0 nm for **3** and 337.0 nm for **4**. In this case, the pyrene shift proved to be similar to the one corresponding to the formation of micelles (band 2, blue) suggesting that at this concentration Av is able to bind with amphiphilic bile acids without micelle disruption. DLS of the above samples 1 and 2 confirmed the spectrofluorimetric data. For example, in the first sample of BBAA **4**, corresponding to band 3 in Fig. 4, unorganized small aggregates were observed as a consequence of micelle disruption due to the excess of Av used in the experiment. DLS of the second sample revealed the presence of larger aggregates (800 nm), which could be interpreted in terms of multimicelle agglomeration induced by tetrameric Av bridging.

Finally, to preliminarily assess whether micelles derived from our BBAA could be uptaken by hepatocyte cells, a murine hepatic cell line was incubated with the different compounds using a concentration high enough to allow the formation of stable micelles. As a proof of concept, for this experiment we selected BBAA **4**, derived from lithocholic acid. As shown in Fig. 5, incubation with **4** resulted in an efficient uptake of BBAA

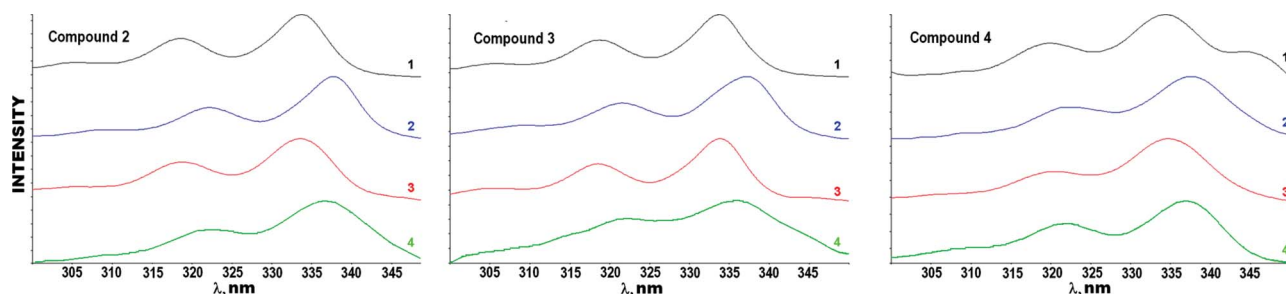


Fig. 4 Pyrene excitation spectra of compounds **2–4** in presence of Av: band 1 (black) pyrene shift without micelles formation; band 2 (blue) pyrene shift with micelles formation; band 3 (red) pyrene shift with 1 : 20 Av/bt ratio; band 4 (green) pyrene shift with 1 : 100 Av/bt ratio.

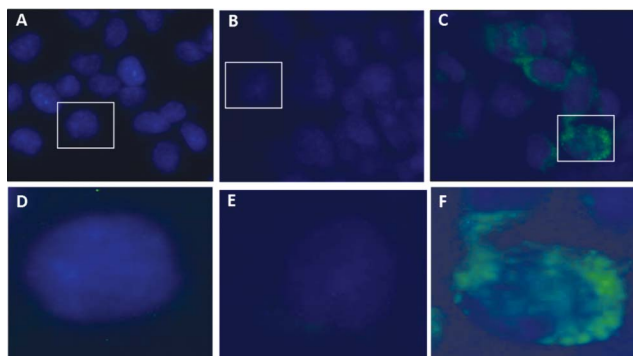


Fig. 5 Bile acid amphiphilic molecules uptake in Hepatic cells. A representative panel of (A) Hepa 1–6 cells under basal conditions, (B) upon incubation with biotin only, and (C) incubated with a bile acid amphiphilic molecule compounds. A magnification of the squared box is presented in D to F, respectively. Nuclei were stained with DAPI (blue signal) and bt was revealed following FITC-streptavidin staining (green signal).

compared to cells under basal conditions (free biotin was used as control). Indeed, FITC-labeled SA_v fluorescence was detected in treated cells.

Conclusions

In summary, we have described a series of amphiphilic molecules (1–4), obtained from biocompatible scaffolds, designed for liver drug targeting, characterized by a biotin moiety linked through an OEG-8 to four different bile acid sources (CA, DCA, UDCA, LA, respectively). Out of them, 2–4 proved to make micellar structures efficiently in aqueous solution. Moreover, all compounds were able to interact with avidin and, in particular, 2–4 were demonstrated to bind with avidin in the form of micelles. Preliminary *in vitro* data showed that such micelles could be efficiently incorporated into hepatic cells and still be able to be targeted by labeled streptavidin. Because of their characteristics of biocompatibility, water solubility and ease of preparation, these synthetic nanoscale vectors can be excellent starting materials for the development of new delivery vehicles for the diagnosis and treatment of liver diseases.

Experimental

Materials and apparatus

Chemicals and solvents were purchased from Iris Biotech (Marktredwitz, Germany), Sigma–Aldrich (Schnellendorf, Germany) and Alfa Aesar (Karlsruhe, Germany) and used without further purifications. Avidin was purchased from Apollo Scientific (Stockport, England). Thin layer chromatography (TLC) was performed using Al-backed sheets coated with silica gel 60F₂₅₄ purchased from Merck (Darmstadt, Germany); spots were further evidenced by phosphomolibdic acid (2% in ethanol). NMR spectra were performed by using a Varian Mercury 300VX. ESI-MS was performed by using a LTQ XL-Orbitrap mass spectrometer (Thermo Scientific, Milan, Italy) with electrospray interface. Capillary electrophoresis (CE) experiments were carried out by using a Beckman Coulter ProteomeLab PA 800. Spectrophotometric measurements were performed by a Perkin-Elmer LAMBDA-11.

Fluorimetric measurements were performed by a Perkin-Elmer LS 50 B. TEM images of nanoparticles were obtained by a Zeiss EM-109 microscope (Oberkochen, Germany) operating at 80 kV. Dynamic Light Scattering (DLS) measurements were performed at 90° with a 90 Plus Particle Size Analyzer from Brookhaven Instrument Corporation (Holtville, NY) working at 15 mW of a solid-state laser ($\lambda = 661$ nm). Hepatocytes images were acquired with a Zeiss Axiovert 200 fluorescence microscope.

General procedures for the synthesis of biotinylated bile acid amphiphiles

OH protection. To a 0.1 M solution of cholic acid or derivatives in dioxane, *p*-toluenesulfonic acid (0.1 eq.) and dihydropyran (1 eq. per OH to be protected) were added. The reaction mixture was stirred, at room temperature, for 30 min. At the end of reaction (TLC monitoring), water (20 mL) was added and the solution was concentrated *in vacuo*. The aqueous phase was extracted with ethyl acetate (3 times) and the collected organic phases were washed with brine (2 times), dried with anhydrous sodium sulfate and concentrated *in vacuo*. The crude product was purified by flash chromatography (DCM–MeOH).

Esterification. To a 1 M solution of protected cholic acid or derivatives in DCM, alcohol (1 eq.), TBTU (1.2 eq.) and DMAP (2 eq.) were added. The reaction mixture was stirred, at room temperature, overnight. At the end of reaction (TLC monitoring), the reaction mixture was evaporated *in vacuo* and the crude product was purified by flash chromatography (DCM–MeOH).

Deprotection. To a 0.1 M solution of protected BBAA in THF a solution of AcOH–THF–water (4 : 2 : 1, 1 mL for mg of protected compound) was added. The reaction mixture was stirred, at 40 °C, for 2 h. At the end of reaction (TLC monitoring) the mixture was neutralized with NaHCO₃, filtered and evaporated *in vacuo*. The crude product was purified by flash chromatography (DCM–MeOH).

CE analysis. The final products were applied to a CE to verify their purity: injections were performed in the hydrodynamic mode (10 s., 0.5 psi) with a running buffer at pH = 2.5 (50 mM phosphate). The capillary (32 cm overall length, 21 cm effective length, 50 μ m i.d.) was operated at 8 kV, while maintaining its temperature at 25 °C; detection was carried out at 220 nm.

Compound 1. 25-oxo-28-(3,7,13-trihydroxy-10-methylhexadecahydro-1H-cyclopenta[a]phenanthren-17-yl)-3,6,9,12,15,18,21,24-octaoxonacosyl-5-(2-oxohexahydro-1H-thieno[3,4-d]imidazol-4-yl)pentanoate was synthesized from cholic acid (500 mg, 1.22 mmol) by OH protection, esterification and OH deprotection protocols, as described above. Colourless oil (21.5 mg, 0.022 mmol). *R_f* 0.6 (DCM–MeOH, 90 : 10). ¹H-NMR (300 MHz, CD₃OD) δ ppm: 4.63–4.54 (t, 1H), 4.42–4.33 (t, 1H), 4.26–4.19 (m, 4H), 3.78–3.41 (m, 28H), 2.95–2.89 (dd, 2H), 2.80–2.73 (t, 2H), 2.42–2.14 (m, 35H), 0.67 (s, 3H). MS (ESI) *m/z*: [M+H]⁺ found 987.60; Calcd: 987.57. CE migration time: 3.51 min.

Compound 2. 28-(3,13-dihydroxy-10-methylhexadecahydro-1H-cyclopenta[a]phenanthren-17-yl)-25-oxo-3,6,9,12,15,18,21,24-octaoxonacosyl-5-(2-oxohexahydro-1H-thieno[3,4-d]imidazol-4-yl)pentanoate was synthesized starting from deoxycholic acid

(500 mg, 1.27 mmol) by using OH protection, esterification and OH deprotection protocols, as described above. Colourless oil (26 mg, 0.030 mmol). R_f 0.43 (DCM–MeOH, 90 : 10). $^1\text{H-NMR}$ (300 MHz, CD_3OD) δ ppm 4.56–4.49 (t, 1H), 4.37–4.26 (t, 1H), 4.24–4.12 (m, 4H), 3.78–3.47 (m, 28H), 2.97–2.89 (dd, 2H), 2.75–2.64 (t, 2H), 2.41–2.21 (m, 6H), 1.98–0.90 (m, 35H), 0.71 (s, 3H). MS (ESI) m/z : $[\text{M}+\text{H}]^+$ found 971.67; Calcd: 971.58. CE migration time: 3.60 min.

Compound 3. 28-(3,7-dihydroxy-10,13-dimethylhexadecahydro-1H-cyclopenta[a]phenanthren-17-yl)-25-oxo-3,6,9,12,15,18,21,24-octaaxanacosyl-5-(2-oxohexahydro-1H-thieno[3,4-d]imidazol-4-yl)pentanoate was synthesized starting from ursodeoxycholic acid (500 mg, 1.27 mmol) by using OH protection, esterification and OH deprotection protocols, as described above. Colourless oil (26 mg, 0.027 mmol). R_f 0.2 (DCM–MeOH, 95 : 5). $^1\text{H-NMR}$ (300 MHz, CD_3OD) ppm 4.64–4.59 (t, 1H), 4.53–4.48 (t, 1H), 4.31–4.16 (m, 4H), 3.73–3.54 (m, 28H), 2.95–2.89 (dd, 2H), 2.80–2.73 (t, 2H), 2.38–2.16 (m, 6H), 1.98–0.68 (m, 35H), 0.64 (s, 3H). MS (ESI) m/z : $[\text{M}+\text{H}]^+$ found 971.80; Calcd: 971.58. CE migration time: 3.62 min.

Compound 4. 28-(3-hydroxy-10,13-dimethylhexadecahydro-1H-cyclopenta[a]phenanthren-17-yl)-25-oxo-3,6,9,12,15,18,21,24-octaaxanacosyl-5-(2-oxohexahydro-1H-thieno[3,4-d]imidazol-4-yl)-pentanoate was synthesized starting from lithocholic acid (500 mg, 1.33 mmol) by using OH protection, esterification and OH deprotection protocols, as described above. Colourless oil (30 mg, 0.03 mmol). R_f 0.55 (DCM–MeOH, 90 : 10). $^1\text{H-NMR}$ (300 MHz, CD_3OD) ppm 4.49–4.47 (t, 1H), 4.33–4.29 (t, 1H), 4.23–4.18 (m, 4H), 3.74–3.55 (m, 28H), 2.96–2.90 (dd, 2H), 2.73–2.69 (t, 2H), 2.49–2.18 (m, 6H), 1.91–0.94 (m, 35H), 0.69 (s, 3H). MS (ESI) m/z : $[\text{M}+\text{H}]^+$ found 955.67; Calcd: 955.59. CE migration time: 3.63 min.

Micelles formation. Compounds were dissolved in THF and HPLC water (3 mL) was added to the solution. Then, THF was removed on a rotary evaporator at 30 °C for 2 h. The aqueous solution was diluted to obtain a concentration range from 5 g L⁻¹ to 10⁻⁴ g L⁻¹. For the measurement of fluorescence spectra, pyrene solution in THF (1.2 × 10⁻³ M) was diluted with HPLC-water to give a pyrene concentration of 12 × 10⁻⁷ M. THF was removed *in vacuo* to obtain a 6 × 10⁻⁷ M pyrene solution, which was mixed to compound samples to obtain final concentrations from 2.5 g L⁻¹ to 5 × 10⁻⁵ g L⁻¹. All the samples were sonicated for 10 min and allowed to stand for 1 day before fluorescence measurement.

Fluorescence measurement. Pyrene was used as fluorescence probe to analyze the compounds in the HPLC-water. For the measurement of pyrene excitation spectra, emission and excitation slit width was set at 2 nm. Excitation spectra measurement was done at $\lambda_{\text{em}} = 393$ nm and the spectra were accumulated with an integration of 20 nm min⁻¹.²²

Avidin-Biotin bond. To 2 mL of avidin solution (1 mg protein in 0.1 M phosphate buffer at pH = 6) was added 4-hydroxyazobenzene-2'-carboxylic acid (HABA, 10 mM in NaOH 0.01 M, 50 μL). UV absorption was measured at 500 nm. Then biotin or biotinylated compounds 1–4 (2 mM in 0.1 M phosphate buffer, 50 μL) were added and absorption was measured at 500 nm

(λ_{max} of Avidin-HABA complex). The occupied avidin binding sites concentration $[\text{bs}]$ was calculated from the following relationship:

$$[\text{bs}] = \frac{\Delta A_{500}}{34} \text{mM}$$

where ΔA_{500} is the difference between absorptions with and without biotinylated compounds and 34 is the extinction coefficient of the avidin-HABA complex at 500 nm.²⁸

Cell culture, *in vitro* uptake and visualization of bile acids amphiphilic molecules

The murine hepatoma cell line Hepa 1–6 was grown in High glucose Dulbecco's modified Eagle medium (DMEM) supplemented with 10% Foetal bovine serum (FBS), 2 mM L-glutamine and 100 units mL⁻¹ of penicillin and 100 $\mu\text{g mL}^{-1}$ of streptomycin. Cells were grown on gelatin coated glass slides in a 24-well plate until 70% confluence, then the media was removed and cells were incubated with bile acid amphiphilic molecule 4 at a concentration of 0.5 mg mL⁻¹ in FBS free medium for 6 h at 37 °C. Cells were rinsed three times with ice cold PBS and fixed with 4% paraformaldehyde for 15 min at room temperature. Cells were rinsed once more with PBS and membranes were permeabilized with 0.2% Triton X-100 in PBS then cells were incubated with FITC conjugated streptavidin (1 : 200 in PBS) to detect biotin conjugated micelles and with DAPI (diamidino-2-phenylindole) for nuclear staining.

Acknowledgements

This work was supported by PRIN 2008 (Leads ad Attività Antimalarica di Origine Naturale: Isolamento, Ottimizzazione e Valutazione Biologica), CMENA and “Fondazione Romeo ed Enrica Invernizzi”.

References

- 1 R. Satchi-Fainaro, M. Puder, J. W. Davies, H. T. Tran, D. A. Sampson, A. K. Greene, G. Corfas and J. Folkman, *Nat. Med.*, 2004, **10**, 255–261.
- 2 B. G. De Geest, G. B. Sukhorukov and H. Moehwald, *Expert Opin. Drug Delivery*, 2009, **6**, 613–624.
- 3 P. Crosasso, M. Ceruti, P. Brusa, S. Arpicco, F. Dosio and L. Cattel, *J. Controlled Release*, 2000, **63**, 19–30.
- 4 K. Greish, T. Sawa, J. Fang, T. Akaike and H. Maeda, *J. Controlled Release*, 2004, **97**, 219–230.
- 5 W. Y. Yu and N. Zhang, *Curr. Nanosci.*, 2009, **5**, 123–134.
- 6 M. Das, C. Mohanty and S. K. Sahoo, *Expert Opin. Drug Delivery*, 2009, **6**, 285–304.
- 7 L. Serfaty and M. Lemoine, *Diabetes Metab.*, 2008, **34**, 634–637.
- 8 Y. Horsmans, *Expert Opin. Pharmacother.*, 2010, **11**, 571–577.
- 9 W. L. Tsai and R. T. Chung, *Oncogene*, 2010, **29**, 2309–2324.
- 10 P. J. Meier and B. Stieger, *Annu. Rev. Physiol.*, 2003, **64**, 635–661.
- 11 A. Balakrishnan, S. A. Wring, A. Coop and J. E. Polli, *Mol. Pharmaceutics*, 2006, **3**, 282–292.
- 12 C. Kim, S. C. Lee, S. W. Kang, I. C. Kwon, Y. H. Kim and S. Y. Jeong, *Langmuir*, 2000, **16**, 4792–4797.
- 13 G. Putz, W. Schmider, R. Nitschke, G. Kurz and H. E. Blum, *J. Lipid Res.*, 2005, **46**, 2325–2338.
- 14 O. F. W. James, *J. Hepatol.*, 1990, **11**, 5–8.
- 15 M. Watanabe, S. Hanashima, Y. Mizushima, H. Yoshida, M. Oshige, K. Sakaguchi and F. Sugawara, *Bioorg. Med. Chem. Lett.*, 2002, **12**, 287–290.
- 16 A. N. Lukyanov and V. P. Torchilin, *Adv. Drug Delivery Rev.*, 2004, **56**, 1273–1289.
- 17 K. F. Pirollo and E. H. Chang, *Trends Biotechnol.*, 2008, **26**, 552–558.

-
- 18 Y. Bae and K. Kataoka, *Adv. Drug Delivery Rev.*, 2009, **61**, 768–784.
- 19 R. Pellicciari, G. Costantino, E. Camaioni, B. M. Sadeghpour, A. Entrena, T. M. Willson, S. Fiorucci, C. Clerici and A. Gioiello, *J. Med. Chem.*, 2004, **47**, 4559–4569.
- 20 K. Kalyanasundaram and J. K. Thomas, *J. Am. Chem. Soc.*, 1977, **99**, 2039–2044.
- 21 M. Wilhelm, C. L. Zhao, Y. Wang, R. Xu, M. A. Winnik, J. L. Mura, G. Riess and M. D. Croucher, *Macromolecules*, 1991, **24**, 1033–1040.
- 22 S. C. Lee, Y. K. Chang, J. S. Yoon, C. H. Kim, I. C. Kwon, Y. H. Kim and S. Y. Jeong, *Macromolecules*, 1999, **32**, 1847–1852.
- 23 J. Luo, K. Xiao, Y. Li, J. S. Lee, L. Shi, Y.-H. Tan, L. Xing, R. H. Cheng, G.-Y. Liu and K. S. Lam, *Bioconjugate Chem.*, 2010, **21**, 1216–1224.
- 24 W.-Q. Chen, H. Wei, S.-L. Li, J. Feng, J. Nie, X.-Z. Zhang and R.-X. Zhuo, *Polymer*, 2008, **49**, 3965–3972.
- 25 K. Zhang, Y. Wang, A. Yu, Y. Zhang, H. Tang and X. X. Zhu, *Bioconjugate Chem.*, 2010, **21**, 1596–1601.
- 26 D. Madenci and S. U. Egelhaaf, *Curr. Opin. Colloid Interface Sci.*, 2010, **15**, 109–115.
- 27 D. A. Goodwin and C. F. Meares, *Biotechnol. Adv.*, 2001, **19**, 435–450.
- 28 N. M. Green, in *Methods Enzymol.*, ed. B. M. Donald and D. W. Lemuel, Academic Press, 1970, vol. Volume 18, Part 1, pp. 418–424.
- 29 N. M. Green, *Biochem. Biophys. Res. Commun.*, 1963, 585.